Purinergic Signalling (2009) 5:351–368
DOI 10.1007/s11302-009-9161-3

ORIGINAL ARTICLE

$P2X_7$ receptor expression is decreased in epithelial cancer cells of ectodermal, uro-genital sinus, and distal paramesonephric duct origin

Xin Li · Xiaoping Qi · Lingyin Zhou · Wen Fu · Fadi W. Abdul-Karim · Gregory MacLennan · George I. Gorodeski

Received: 31 October 2008 / Accepted: 6 April 2009 / Published online: 28 April 2009

Abstract The $P2X_7$ receptor is an important regulator of epithelial cell growth. The aim of the present study was to better understand the biological significance of $P2X_7$ receptor expression in normal and cancer human epithelial tissues. $P2X_7$ receptor and messenger RNA (mRNA) levels were determined in human tissues containing epithelial dysplastic, pre- or early cancerous, and cancer cells, and the levels were compared to those in the corresponding normal epithelial cells within the same tissue of the same case. $P2X_7$ receptor levels were determined by quantification of immunoreactivity specific to the functional (full-length) $P2X_7$ receptor, and $P2X_7$ mRNA levels were determined by real-time polymerase chain reaction. $P2X_7$ receptor levels in cancer cells were similar (colon adenocarcinoma) or greater (thyroid papillary carcinoma) than those in the corresponding normal cells. In contrast, in cancer cells of the ectocervix (squamous), endocervix and endometrium (adenocarcinoma), urinary bladder (transitional cell carcinoma), and breast (ductal and lobular adenocarcinomas), $P2X_7$ receptor levels were lower by about twofold than those in the corresponding normal epithelial cells. Similarly, $P2X_7$ mRNA levels were lower in uterine, bladder, and breast cancer epithelial tissues by about fourfold than those in the corresponding normal tissues. In addition, $P2X_7$ receptor levels were decreased already in dysplastic ectocervical cells and pre- or early cancerous endometrial and bladder cells. The data suggest that in epithelia originating from the ectoderm, the uro-genital sinus, and the distal paramesonephric duct, decreased expression of the $P2X_7$ receptor precedes or coincides with neoplastic changes in those tissues.

Keywords $P2X_7$ · Epithelium · Epithelia · Normal · Cancer

X. Li (✉)
Department of Pathology, University of Toledo Medical Center,
3000 Arlington Avenue,
Toledo, OH 43614, USA
e-mail: xin.li@utoledo.edu

X. Qi · L. Zhou · W. Fu · G. I. Gorodeski (✉)
Department of Reproductive Biology,
Case Western Reserve University,
11100 Euclid Avenue,
Cleveland, OH 44106, USA

F. W. Abdul-Karim · G. MacLennan
Department of Pathology, Case Western Reserve University,
Cleveland, OH, USA

G. I. Gorodeski
Department of Oncology, Case Western Reserve University,
Cleveland, OH, USA

G. I. Gorodeski
Department of Physiology and Biophysics,
Case Western Reserve University,
Cleveland, OH, USA

Introduction

The main cellular mechanism that controls growth of epithelial cells is apoptosis. Apoptosis is a regulated homeostatic process orchestrated by the host's genome of selective cell deletion without stimulating inflammatory response [1–3]. Although apoptosis can be activated in response to noxious stimuli, e.g., starvation, inflammation, infection, and irradiation, recent data suggest an active physiological role for apoptosis. These include the control of tissue development and differentiation, regulation of mitogenic effects, and control of cell death and loss of tissue with aging [4]. Dysregulation of apoptotic cell death

has been implicated in states of disease and in the neoplastic transformation [1–5].

Among the pro-apoptotic systems that operate in epithelial tissues [6], the $P2X_7$ mechanism is probably the most important because the $P2X_7$ receptor is expressed mainly by proliferating epithelial cells [7], thereby controlling directly the growth of epithelia. The $P2X_7$ receptor is a membrane-bound, ligand-operated channel whose main function in epithelial cells is mediation of apoptosis [8–10]. The natural ligand of the $P2X_7$ receptor is adenosine triphosphate (ATP) [8, 9], which is present in the extracellular fluid of epithelial cells at high nanomolar and low micromolar levels [11–15]. While ATP requirements of the $P2X_7$ receptor are higher than those of other purinergic receptors [8, 9], the ATP levels in extracellular fluids suffice to activate the receptor [15]. Activation by ATP can stimulate different signaling pathways including the IL-1β [16], TNFα–TRAIL [17], and the p38, JNK/SAPK [18], and NF-κB cascades [19], some of which can induce apoptosis. The quantitatively significant pro-apoptotic ATP/$P2X_7$ effect in epithelial cells involves formation of pores in the plasma membrane [6, 15, 20], and uncontrolled influx of Ca^{2+} via $P2X_7$ pores induces apoptosis by the mitochondrial–caspase-9 pathway [6, 15].

$P2X_7$ pore formation involves formation of channels composed of pannexins [21, 22] and ectodomains of the $P2X_7$ molecule [20, 23], and it depends on ligand (ATP) availability, expression in the plasma membrane of the functional (glycosylated) full-length receptor, homo(tri)-oligomerization of the functional full-length receptor [8–10], and the presence of $P2X_7$ splice variants [20]. $P2X_7$ molecules can hetero-oligomerize with other types of P2 purinergic receptor molecules [24], but it is unknown whether these interactions result in the formation of pores. In contrast, $P2X_7$ molecules can hetero-oligomerize with truncated and other $P2X_7$ splice variant molecules, thereby forming non-functional oligomers that prevent formation of functional pores [20].

Central to the ability of ATP to induce apoptosis via the $P2X_7$ pore mechanism is the degree of cellular expression of the $P2X_7$ receptor [10]. Plasma membrane expression of the $P2X_7$ receptor depends on the rates of transcription and $P2X_7$ messenger RNA (mRNA) degradation [25]; receptor glycosylation [26, 27], trafficking, and sorting to the plasma membrane [26]; and on receptor turnover as determined by internalization, degradation, and recycling [26]. Ligand-dependent activation of the receptor induces GRK-3, β-arrestin-2, dynamin-dependent internalization into clathrin domains, and receptor recycling into the plasma membrane [26].

The question of $P2X_7$ receptor expression in cancer epithelial cells and whether changes in expression play a role in cancer development were raised already a decade ago (e.g., [28]), usually in the context of biomarker research (e.g., [29]). Earlier studies reported lower levels of the receptor in non-melanoma skin cancer than in normal tissues [28], but higher levels of the receptor in breast cancers [30] melanoma [29] and prostate cancers [31] than in normal tissues. However, the significance of these findings is unclear since some of the studies used methods that could have detected non-functional $P2X_7$ receptors. For instance, Barden et al. [29–32] assayed $P2X_7$ immunoreactivity with rabbit anti-$P2X_7$ antibody raised against epitope C200-C216 of the human $P2X_7$ receptor. This epitope is located in the extracellular loop of the protein, and the antibody is likely to detect both the full-length functional receptor as well as variants lacking the C-terminus [20], which is critical for $P2X_7$ mediation of apoptosis [20]. Variants lacking the C-terminus are non-functional [20], and since the expression of some variants lacking the C-terminus is exceptionally high in cancer cells [20], assays using that antibody may have overestimated expression of the $P2X_7$ receptor in cancer cells by detecting predominantly non-functional receptors.

Recent studies employing methods that used anti-$P2X_7$ antibodies raised against epitopes located in the C-terminus showed lower $P2X_7$ expression and lesser $P2X_7$-dependent apoptosis in uterine epithelial cancer cells than in normal uterine epithelial cells [7, 20, 25, 33]. But a more recent study reported higher levels of the $P2X_7$ receptor in thyroid papillary cancer cells than in normal thyroid cells [34].

In view of the importance of apoptosis-related mechanisms for epithelial cancer development [35–37] and the discrepancy in reports of $P2X_7$ receptor levels in epithelial cancer cells among different studies, a comprehensive study was undertaken to answer some of these questions. The main objective of the study was to improve our understanding of the biological role of the $P2X_7$ in the genesis and development of epithelial cancers. The principles of the study were as follows: (a) detection of $P2X_7$ receptor by immunostaining, using a commercially available, well-characterized anti-$P2X_7$ receptor antibodies that react with the functional $P2X_7$ receptor; (b) quantification of $P2X_7$ receptor immunofluorescence in preserved tissues, in situ, by image capturing and analysis; (c) comparison of $P2X_7$ receptor levels in epithelial cancer cells with those of the corresponding epithelial normal cells of the same tissue in the same surgical specimen (i.e., the same patient); (d) comparison of data obtained by $P2X_7$ receptor immunofluorescence with the data obtained by $P2X_7$ receptor horseradish peroxidase (HRP) immunostaining with diaminobenzidine (DAB); (e) for selected types of epithelial cancers, analysis of $P2X_7$ receptor levels in dysplastic, precancerous, and early stages of the cancer and comparison with the levels in the normal cells of the same surgical specimen; and (f) for selected types of epithelial cancers,

confirmation of the $P2X_7$ receptor (protein) findings with $P2X_7$ mRNA assays.

Experimental procedures

Human tissues

Discarded human tissues for $P2X_7$ receptor (protein) assays were obtained after approval of the research protocol by the Institutional Review Boards from the Human Tissue Procurement Facility of University Hospital CASE Medical Center, Case Western Reserve University, Cleveland, Ohio, and the University of Toledo Medical Center, Toledo, Ohio. Cross sections of tissue segments were obtained from paraffin-embedded blocks that were prepared by the Departments of Pathology initially to establish the patient's diagnosis. For the purpose of the present study, additional parallel 5-μm sections were cut and slides intended for immunostaining were made by the Departments of Pathology according to standard procedures. This part of the study included tissues obtained from 88 patients (72 women and 16 men; Table 1). Included in each case were cross sections of the cancer tissue and an adjacent histologically normal tissue.

Discarded human tissues for mRNA assays were obtained after approval of the research protocol by the Institutional Review Board from the Department of Pathology at the Ohio State University, Columbus, Ohio, through the Cooperative Human Tissue Network (National Cancer Institute). Tissues were snap-frozen in liquid N_2, shipped on dry ice, and stored at −80°C until assayed. Included were tissues obtained from 19 patients (18 women and one man; Table 1). Included in each case were blocks of the cancer tissue and an adjacent histologically normal tissue.

The histological diagnoses presented below were made by the Departments of Pathology at the University Hospital CASE Medical Center, the University of Toledo Medical Center, and the Ohio State University and were provided to the research team prior to assays. No attempt was made to categorize results by patients' gender, age, or ethnic and race origin.

Protein methods

The receptor $P2X_7$ was detected immunologically as described [7, 33], using either the Alomone rabbit polyclonal anti-$P2X_7$ receptor antibody (Alomone Laboratories, Jerusalem, Israel) [7, 20, 25–27, 33] or the rabbit anti-$P2X_7R$ Sigma antibody (Sigma Chemical, St. Louis, MO, USA, Cat # P-8232, Lot # 047K1346), in the absence or presence of the antigen peptide. Both antibodies were raised against an immunogenic peptide corresponding to amino acids 576–595 of the rat $P2X_7$ (with an additional N-terminal cysteine), which represents an epitope that is highly conserved in mouse and human $P2X_7$ [38, 39]. Both antibodies target immunogenic domains at the C-terminus of the receptor and recognize the functional full-length $P2X_7$ receptor [20]. Previous immunostaining studies using the Alomone or Sigma rabbit polyclonal anti-$P2X_7$ receptor antibodies in cultured epithelial cells [6, 7, 15, 20, 26, 27] and in vivo [7, 33] revealed that both antibodies immunoreacted with the functional full-length $P2X_7$ receptor, including the glycosylated (85 kDa) and non-glycosylated forms (65 and 75 kDa). The choice of the antibody was made based on availability, and the results with either

Table 1 Composition of the human tissues used in the study

Organ	Histology	Number of samples (patients)	
		Protein assays	mRNA assays
Ectocervix	Mild-moderate cervical dysplasia	3 (W)	
	Moderate-severe cervical dysplasia	3 (W)	
	Cervical squamous cervical carcinoma	10 (W)	5 (W)
Endocervix	Adenocarcinoma	3 (W)	3 (W)
Endometrium	Simple hyperplasia	5 (W)	
	Complex hyperplasia	3 (W)	
	Complex hyperplasia with atypia	5 (W)	
	Adenocarcinoma	9 (W)	5 (W)
Urinary bladder	Transitional cell carcinoma in situ	4 (W), 8 (M)	
	Transitional cell carcinoma	6 (W), 4 (M)	2 (W), 1 (M)
Breast	Ductal carcinoma	13 (W)	3 (W)
	Lobular carcinoma	3 (W)	
Colon	Adenocarcinoma	3 (W), 2 (M)	
Thyroid	Papillary carcinoma	2 (W), 2 (M)	

W women, *M* men

antibody were similar (not shown). Anti-cytokeratin-18 (CK-18) antibody was from Cell Signaling Technology (Danvers, MA, USA). Anti-E-cadherin antibody was from BD Transduction Laboratories (Lexington, KY, USA). The method of immunostaining was described [7, 33].

For HRP immunostaining with DAB, paraffin tissue cross sections mounted on glass slides were deparaffinized with xylenes, rehydrated with serial ethanols in water (100–0%), washed with phosphate-buffered saline (PBS), and boiled in 10 mM citric acid buffer, pH 6.0 for 10 min. Slides were immersed in 3% bovine serum albumin/1% Triton X-100 for 60 min at room temperature to block non-specific background, and sections were incubated overnight at 4°C in a humidified chamber dark with 1:50 rabbit anti-$P2X_7R$ antibody. Following washes with PBS, sections were incubated with HRP-labeled anti-rabbit IgG (H+L) antibody (Jackson ImmunoResearch Cat # 211-035-109) at 1:500 for 1 h at room temperature in the dark. The reaction was developed using peroxidase substratebkit DAB (Vector, Cat # SK-4100) for 5 min at room temperature; sections were washed with PBS and water, counterstained with hematoxylin for 30 s, washed in water, dehydrated with serial ethanol, and cleared with xylene. Coverslips were mounted using permanent mounting medium, and pictures were captured by light microscopy.

The method of image analysis of immunofluorescence data was described [7, 33]. Briefly, tissue cross sections were analyzed under a fluorescence microscope Nikon Eclipse 80i (Nikon, Melville, NY, USA). Fields of interest were captured and saved in Adobe Photoshop. Pictures were scanned using UN-SCAN-IT software (Silk Scientific, Orem, UT, USA) by choosing three to five representative fields for each picture. Fields of interest were chosen in reference to the epithelial component of the tissue, as determined by co-immunostaining with E-cadherin or CK-18 ([33]; Fig. 1a, b). Light intensity in each field (usually at ×10 magnification) was digitized, and average pixel density for $P2X_7$ per field was determined using the program software. For each clinical case, average data of $P2X_7$ pixel density in the histologically diagnosed abnormal regions were normalized to the average $P2X_7$ pixel density of the histologically diagnosed normal region.

Real-time quantitative polymerase chain reaction

Total RNA from tissues was extracted by RNeasy mini kit (Qiagen, Valencia, CA, USA), and one-step real-time quantitative polymerase chain reaction (qPCR) was carried out as described [33]. Primers for the $P2X_7$, E-cadherin, and CK-18 (for data normalization per epithelial mass) and PCR conditions were described [7, 20, 33]. E-cadherin was used for assays with ectocervical tissues, and CK-18 was used for assays with endocervical, endometrial, bladder, and breast tissues. Relative quantification (RQ) was calculated using Applied Biosystems SDS software (Foster City, CA, USA) based on the equation $RQ = 2^{-\Delta\Delta Ct}$ where C_t is the threshold cycle to detect fluorescence. For each clinical case, $P2X_7$/E-cadherin mRNA or $P2X_7$/CK-18 mRNA levels in the histologically diagnosed abnormal regions were normalized to the $P2X_7$/E-cadherin mRNA or $P2X_7$/CK-18 mRNA levels of the histologically diagnosed normal region (all assays in triplicates).

Data analysis

Data were analyzed using GraphPad Instat, GraphPad Software Inc., San Diego, CA, USA. Significance of differences among groups was estimated by paired *t* test and Mann–Whitney analysis.

Supplies

All chemicals, unless specified otherwise, were obtained from Sigma Chemical (St. Louis, MO, USA).

Results

Validation of the $P2X_7$ immunostaining methods

For immunofluorescence assays, the epithelial component of the tissues was identified by staining with the anti-E-cadherin (or anti-cytokeratin-18) antibodies (Fig. 1a). Co-staining with the anti-$P2X_7$ antibody revealed immunoreactivity localized foremost with the epithelial component of the tissue (Fig. 1b). The $P2X_7$ immunoreactivity was blocked when tissues were co-incubated with the $P2X_7$ antigen (Fig. 1c).

The intensity of the $P2X_7$ immunoreactivity signal differed by the presence of abnormal cells. For instance, in the example of urinary bladder cross section shown in Fig. 1a–c, containing both normal and transitional cell cancer tissues, the anti-$P2X_7$ antibody reacted with both the normal and the cancerous cells. However, the $P2X_7$ immunofluorescence of normal cells was stronger than that of the cancer cells (Fig. 1b), and quantification revealed that the $P2X_7$ immunofluorescence in the cancer cells was weaker, at only 0.55-fold of that in the normal cells.

Data obtained by $P2X_7$ receptor immunofluorescence were compared with those obtained by $P2X_7$ receptor HRP–DAB immunostaining and the results were similar. For example, in the cross section of thyroid tissue shown in Fig. 1e, containing both normal and papillary cancer tissue, the $P2X_7$ immunofluorescence in the cancer cells was 1.35-fold stronger than the $P2X_7$ immunofluorescence in the normal cells. In a parallel section cut from the same

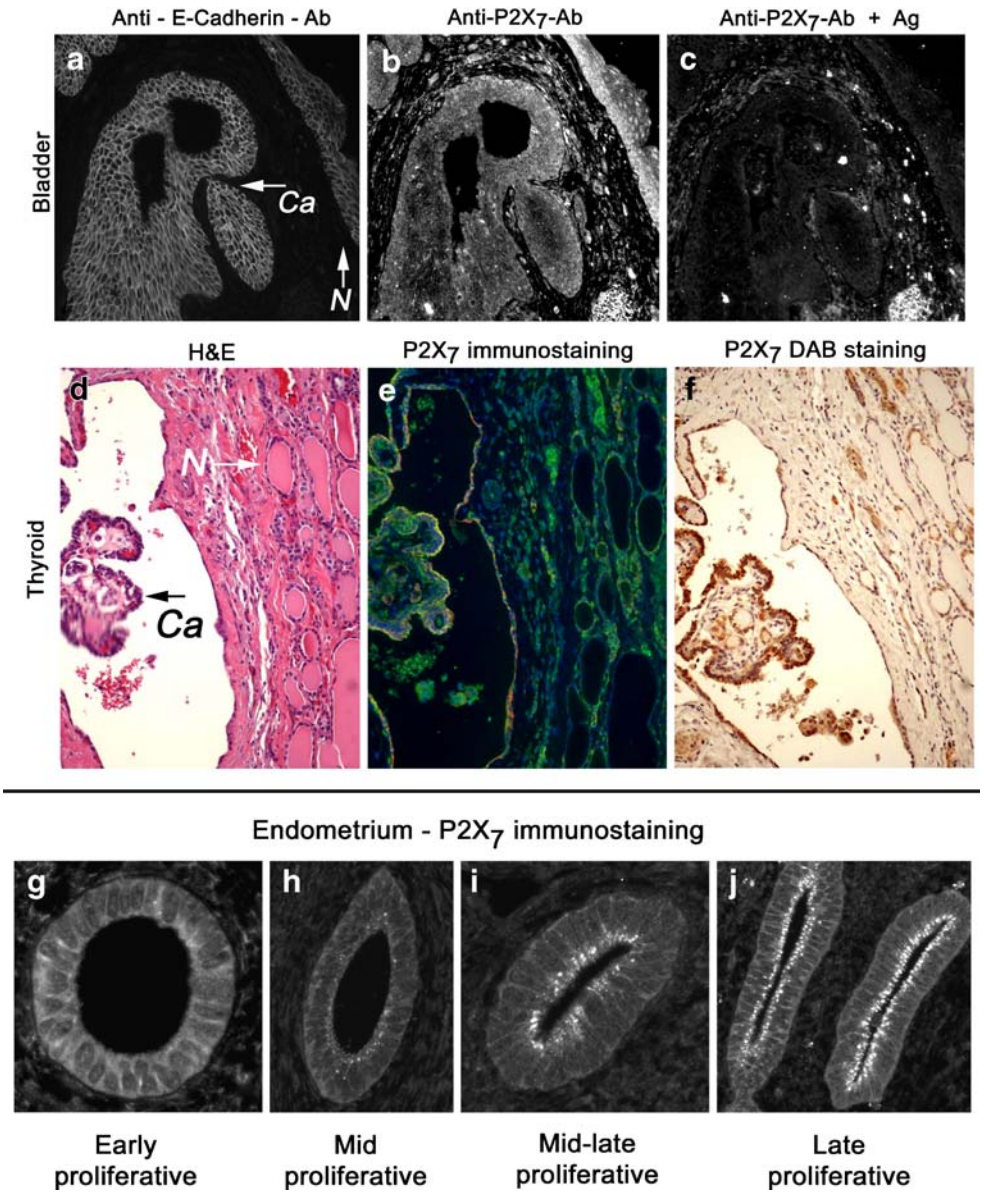

Fig. 1 **a–c** Co-immunostaining of bladder cross section, containing normal (*N*) and transitional cell carcinoma tissues (*Ca*), with anti-E-cadherin antibody (*Ab*; **a**), and anti-$P2X_7$ antibody in the absence (**b**) or presence (**c**) of the $P2X_7$ antigen (*Ag*). The specific $P2X_7$ immunoreactivity of cancer cells was 0.55-fold weaker than that of the normal cells. Magnification ×10. **d–f**. Cross section of thyroid, containing normal (*N*) and papillary carcinoma tissues (*Ca*), stained with H&E (**d**); co-immunostained with anti-$P2X_7$ antibody (*green*), anti-cytokeratin-18 antibody (*red*), and with DAPI (nuclear stain, *blue*) and evaluated by immunofluorescence (**e**); or immunostained with anti-$P2X_7$ antibody by HRP–DAB method (**f**). The $P2X_7$ immunoreactivity of cancer cells in **e** was 1.35-fold stronger than that of the normal cells, and the $P2X_7$ immunoreactivity by HRP–DAB immunostaining showed a similar trend (**f**). Magnification ×10. **g–j** Immunostaining with anti-$P2X_7$ antibody of endometrial glands cross sections obtained from women at different phases of the menstrual cycle. Magnification ×20

specimen, $P2X_7$ receptor HRP–DAB immunostaining showed a similar trend (Fig. 1f). These data validate the specificity of either method to detect $P2X_7$ immunoreactivity in tissue cross sections in situ. However, since immunofluorescence assays proved to have greater sensitivity and the advantage of double staining with an epithelial marker (E-cadherin or CK-18), they were used as the main method for quantification of $P2X_7$ immunoreactivity.

The cellular compartmentalization of the $P2X_7$ immunoreactivity depended on the type of cell that was studied and on its state of differentiation. $P2X_7$ immunoreactivity could be detected at cell regions of the plasma membrane, cytoplasm, perinuclear, and occasionally in nuclear regions (see below). In the example of the uterine epithelium, high magnification of cross sections of early proliferative endometrial glands demonstrated diffuse $P2X_7$ immunoreactivity in the cytoplasm, perinuclear regions, and plasma membranes, with minimal nuclear staining (Fig. 1g). In cross sections of endometrial glands at more advanced stage of maturation (i.e., mid-late proliferative phases), the $P2X_7$ immunoreactivity in apical (luminal) plasma membrane regions increased, while the $P2X_7$ immunoreactivity in the basolateral regions of the plasma membrane and in the cytoplasm and perinuclear regions remained stable (Fig. 1h–j). A similar effect of predominantly apical localization of the $P2X_7$ receptor was described in ectocervical epithelial cells [40]. In contrast, in the colonic epithelium, $P2X_7$ receptor expression was equally distributed in the apical and basolateral regions of the plasma membrane (not shown).

$P2X_7$ receptor levels in normal and cancer epithelial cells

Levels of $P2X_7$ receptor were evaluated in situ in normal and cancer epithelial cells of the following seven tissues: ectocervix, endocervix, endometrium, urinary bladder, breast, colon, and thyroid. In some tissues (ectocervix, endometrium, and bladder), assays evaluated $P2X_7$ receptor levels also in hyperplastic, dysplasia, pre-cancerous, and early stage cancer cells. In all cases, the histological diagnoses were provided to the research team prior to the $P2X_7$ assays. Included in the study were specimens (one per patient) that included both the normal and abnormal tissue, sometimes within the same microscopical field. For each clinical case (i.e., patient), cross sections including the normal and abnormal tissues were mounted on the same glass slide and were assayed simultaneously. Since the focus of the study was to better understand the biological role of the $P2X_7$ in the genesis and development of epithelial cancers rather than biomarker assays, in each clinical case, data of epithelial $P2X_7$ immunoreactivity in abnormal cells were normalized to those of normal cells. Examples of $P2X_7$ receptor immunofluorescence data are shown in Figs. 1, 2, 3, 4, and 5, and of $P2X_7$ receptor HRP–DAB immunostaining in Figs. 1 and 6. Data of $P2X_7$ receptor immunoreactivity are summarized in Fig. 7.

Ectocervix In cross sections of the normal ectocervix, $P2X_7$ immunoreactivity was found mainly in the epithelial cells, and it was prominent in cells of the basal/parabasal layers (i.e., the proliferating cells; e.g., Figs. 2a, e and 6a). The staining was usually weaker in cells of the intermediate layers and stronger in the superficial layers (Figs. 2a, e and 6a). In most cases, staining was found in the cytoplasm and plasma membrane, with moderate nuclear staining (e.g., Fig. 2a). In some cases, the nuclear staining was minimal (e.g., Fig. 2i). In dysplastic and squamous carcinoma cells, the weak $P2X_7$ immunoreactivity was distributed throughout the cell (Fig. 2c, g, and k). Sixteen clinical cases were studied, including three mild-moderate dysplasias, three moderate-severe (high-grade) dysplasias, and ten squamous cell carcinomas (Table 1). Ten cases (all dysplasias and four cancers) were evaluated by $P2X_7$ receptor immunofluorescence, four cancer cases by $P2X_7$ receptor HRP–DAB immunostaining, and one cancer case was evaluated both by the immunofluorescence and HRP–DAB immunostaining methods. In cases of cervical dysplasia, $P2X_7$ receptor levels were lower in dysplastic cells compared to normal cells, regardless of the degree of dysplasia (e.g., Fig. 2a, c, e, and g). In those cases, the mean ratio (± SD) of mild-moderate dysplasia/normal $P2X_7$ receptor levels was 0.46±0.15 (Fig. 7a, $p<0.01$, compared to normal), and the mean ratio of moderate-severe dysplasia/normal $P2X_7$ receptor levels was 0.40±0.18 (Fig. 7b, $p<0.01$). In all cancer cases evaluated by immunofluorescence, epithelial cell $P2X_7$ receptor levels were lower in the cancer cells than in the normal cells (e.g., Fig. 2i, k), and the mean ratio of cancer/normal $P2X_7$ receptor levels was 0.45±0.16 (Fig. 7c, $p<0.01$). Similar results were obtained in the cases that were evaluated by HRP–DAB immunostaining (e.g., Fig. 6a, b).

Endocervix In cross sections of the normal endocervix, $P2X_7$ immunoreactivity was found mainly in epithelial cells composing the endocervical crypt, and it was localized in the cytoplasm and plasma membrane, with minimal-moderate nuclear staining (Fig. 2m). A similar pattern was found in tissues with endocervical adenocarcinoma (Fig. 2o). Three cases of endocervical adenocarcinoma were evaluated by $P2X_7$ receptor immunofluorescence (Table 1). In all cases, epithelial cell $P2X_7$ receptor levels were lower in the cancer cells than those in the normal cells (e.g., Fig. 2m, n), and the mean ratio of cancer/normal $P2X_7$ receptor levels was 0.52±0.07 (Fig. 7d, $p<0.01$).

Endometrium In cross sections of the normal endometrium, $P2X_7$ immunoreactivity was found mainly in epithelial cells composing the endometrial glands (Figs. 3a, e, i, n and 6c, d). Immunoreactivity was found in the cytoplasm and plasma membrane, with minimal nuclear staining, but the most prominent staining was found in apical cytoplasmic/plasma membrane regions of the cells (Figs. 3e, n and 6c, d). A similar pattern was found in tissues with endometrial simple (Fig. 3c) and complex hyperplasia (Fig. 3g). A similar pattern was also found in tissues with endometrial complex hyperplasia with atypia (Fig. 3k) and endometrial adenocarcinoma (Figs. 3n and 6c, d), but the prominent apical glandular hyperstaining was lost. Twenty-two cases were studied, including eight cases of benign hyperplasia (five simple and three complex hyperplasia without atypia), five cases of the pre-cancerous complex hyperplasia with atypia, and nine endometrial carcinomas (all type 1 endometrioid adenocarcinomas; Table 1). Nineteen cases (all benign hyperplastic and pre-cancerous cases and six cancers) were evaluated by $P2X_7$ receptor immunofluorescence; one cancer case was evaluated by the $P2X_7$ receptor HRP–DAB immunostaining method, and one cancer case was evaluated by both the immunofluorescence and HRP–DAB immunostaining methods. In all cases of benign hyperplasia, $P2X_7$ receptor levels were similar to those in normal cells (e.g., Fig. 3a, c, e, and g) with a mean ratio of hyperplasia/normal $P2X_7$ receptor levels of 1.01±0.06 (Fig. 7e, $p>0.8$). In contrast, in all cases of complex hyperplasia with atypia, $P2X_7$ receptor levels were lower in the abnormal cells compared to the normal cells (e.g., Fig. 3i, k), and in those cases, the mean ratio of abnormal/normal $P2X_7$ receptor levels was 0.39±0.10 (Fig. 7f, $p<0.01$). In all cancer cases evaluated by immunofluores-

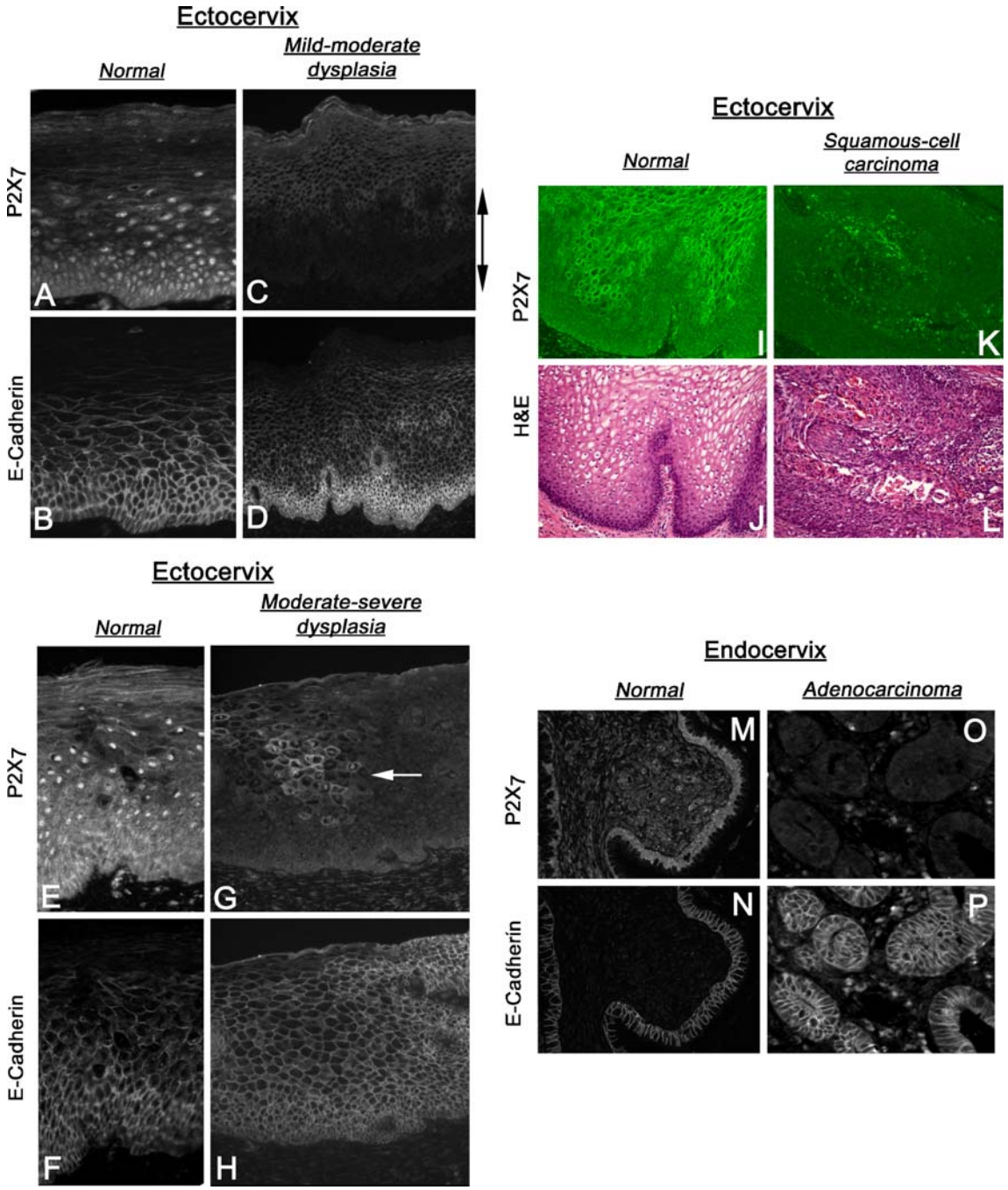

Fig. 2 $P2X_7$ and E-cadherin immunoreactivities (by immunofluorescence) in cross sections of ectocervical normal, dysplasia, and squamous carcinoma tissues (**a–i**, **k**), and of normal and adenocarcinoma endocervical tissues (**m–p**). Each of the four panels (**a–d**, **e–h**, **i–j**, **m–p**) shows normal and dysplasia/cancer tissues obtained from the same patient. **c, d** The dysplasia occupies about one half of the thickness of the epithelium (*double-pointed arrow*). **g**, **h** The dysplasia occupies the entire thickness of the epithelium, engulfing an island of histologically appearing normal granular superficial cells (*left-pointed arrow*). Magnification ×10. Data are summarized in Fig. 7

cence, epithelial cell $P2X_7$ receptor levels were lower in the cancer cells than in the normal cells (e.g., Fig. 3m, n) with a mean ratio of cancer/normal $P2X_7$ receptor levels of 0.40± 0.12 (Fig. 7g, $p<0.01$). Similar results were obtained in cancer cases that were evaluated by HRP–DAB immunostaining (e.g., Fig. 6c, d).

Urinary bladder In cross sections of the normal urinary bladder, $P2X_7$ immunoreactivity was found mainly in the transitional epithelial cells, and it was more prominent in cells resting on the basal membrane (i.e., the proliferating cells; Figs. 1b and 4a). The strongest staining was found in perinuclear regions, but immunoreactivity was also found

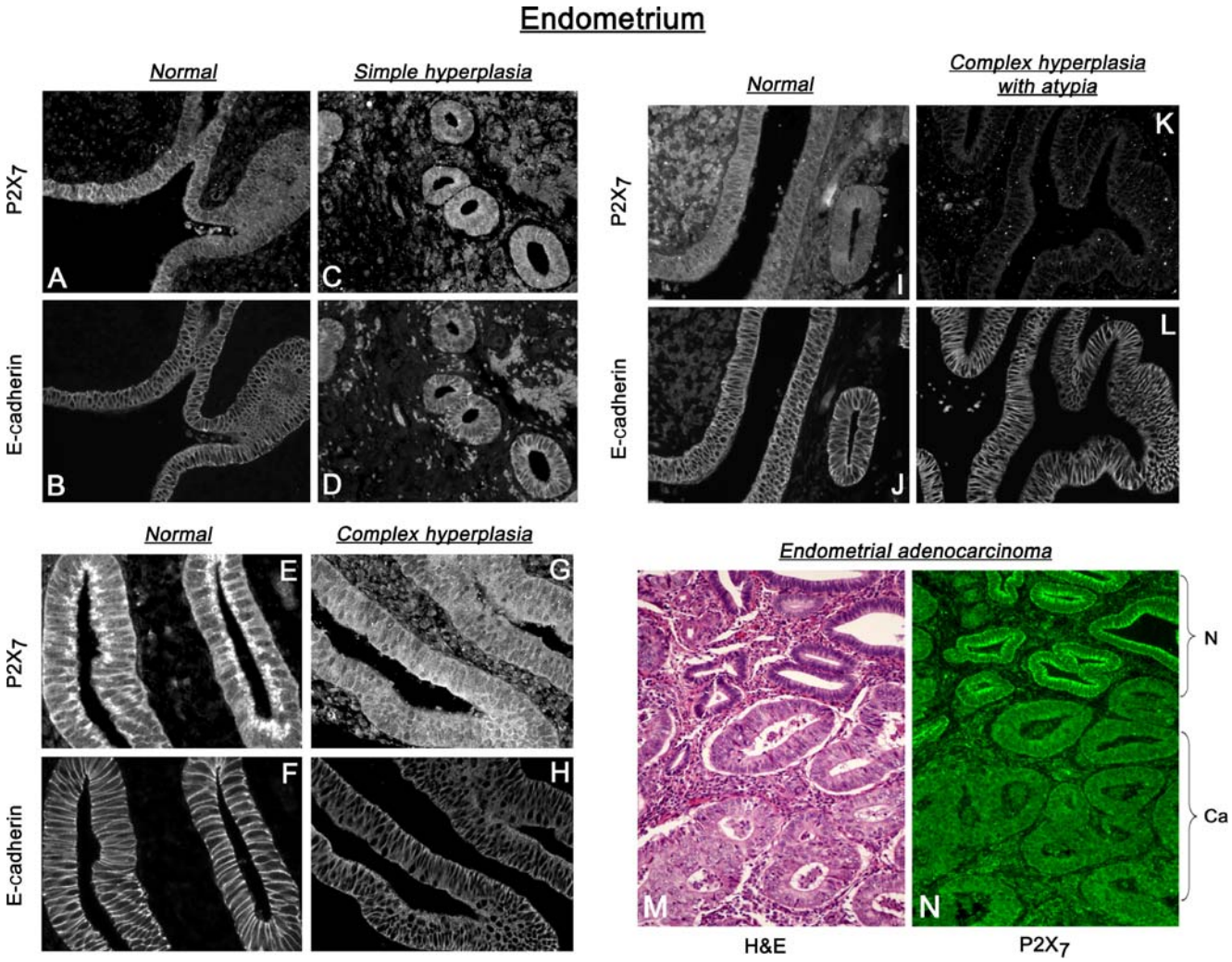

Fig. 3 $P2X_7$ and E-cadherin immunoreactivities (by immunofluorescence) in cross sections of normal endometrium and of endometrium containing simple hyperplasia, complex hyperplasia, complex hyperplasia with atypia, and adenocarcinoma (**a**–**n**). Each of the four panels (**a**–**d**, **e**–**h**, **i**–**l**) shows normal and hyperplasia/cancer tissues obtained from the same patient. **m**, **n** Cross sections containing both normal endometrial glands (*upper part*, *N*) and adenocarcinomatous glands (*lower part*, *Ca*). Magnification ×10. Data are summarized in Fig. 7

in the cytoplasm and plasma membrane, with minimal-moderate nuclear staining. A similar pattern was also found in tissues with transitional cell carcinoma in situ (Fig. 4c, g), and with invasive transitional cell carcinomas (Fig. 4k, o). Twenty-two clinical cases were studied, including ten invasive transitional cell carcinomas, and 12 cases of transitional cell carcinoma in situ (Table 1). All cases were evaluated by $P2X_7$ receptor immunofluorescence immunostaining. In ten of the 12 cases of transitional cell carcinoma in situ, $P2X_7$ receptor levels were lower in the cancer cells than in the normal cells (e.g., Figs. 4a, c, e and 7i), while in two cases $P2X_7$ receptor levels were higher in the carcinoma in situ cells than in the normal cells (Fig. 7i). However, for the entire transitional cell carcinoma in situ group, the mean ratio of cancer/normal $P2X_7$ receptor levels was 0.77±0.15 (Fig. 7i, $p<0.01$). In all cases of invasive transitional cell carcinoma, epithelial cell $P2X_7$ receptor levels were lower in the cancer cells than in the normal cells (e.g., Fig. 4i, k, m, and o), and the mean ratio of cancer/normal $P2X_7$ receptor levels was 0.48±0.15 (Fig. 7j, $p<0.01$).

Breast In cross sections of the normal breast, $P2X_7$ immunoreactivity in ductal and lobular tissues was localized mainly in perinuclear regions and the plasma membrane, with minimal nuclear staining (Fig. 5a, e, and i). In breast ductal or lobular carcinoma cells, the $P2X_7$ immunoreactivity was distributed throughout the cells, with minimal nuclear staining (Fig. 5c, g, and k). Sixteen clinical cases were studied, including 13 invasive ductal carcinomas and three invasive lobular carcinomas (Table 1). Fourteen cases were evaluated by $P2X_7$ receptor immuno-

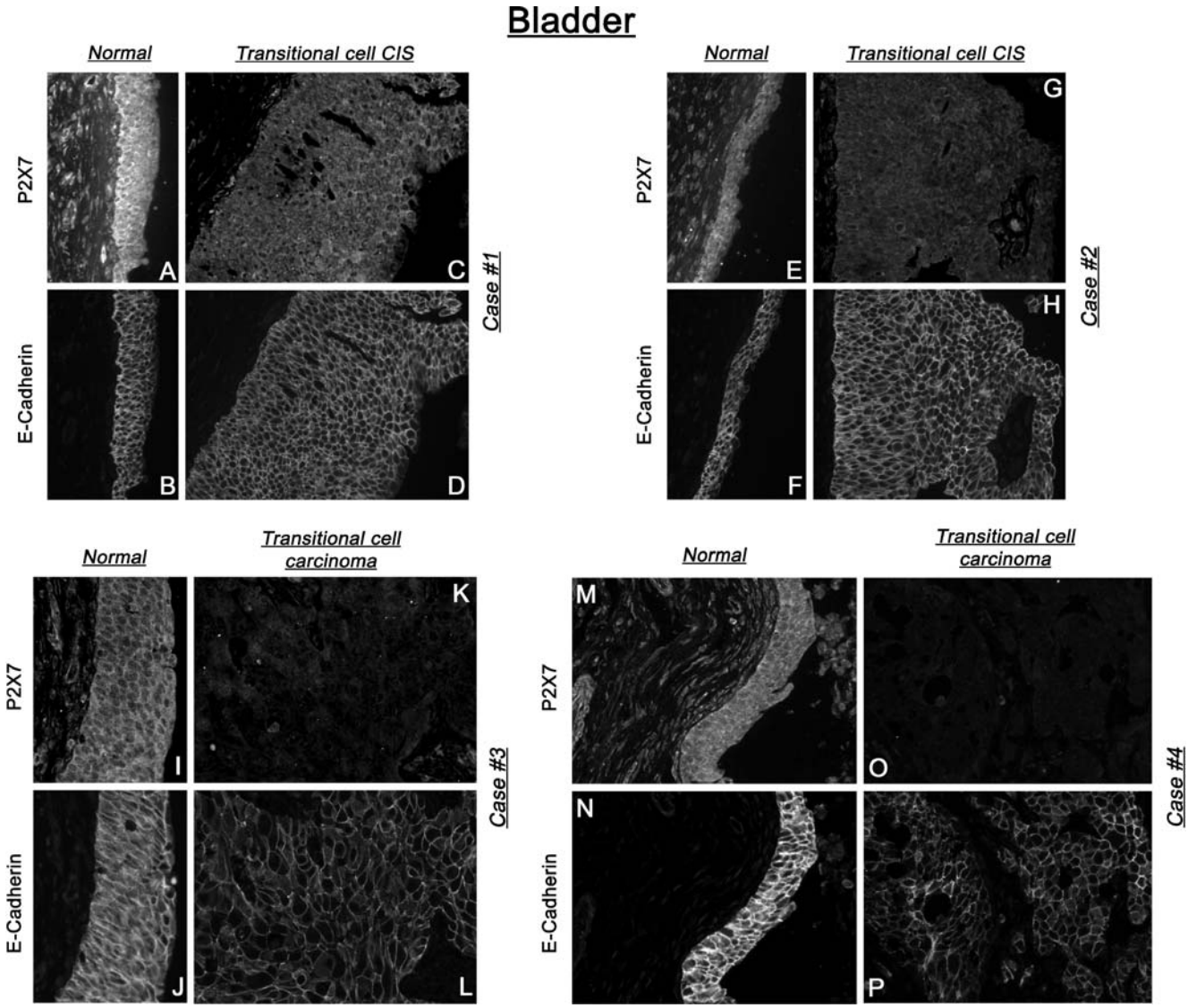

Fig. 4 $P2X_7$ and E-cadherin immunoreactivities (by immunofluorescence) in cross sections of normal urinary bladder and of bladder containing transitional cell carcinoma in situ (*CIS*; cases 1 and 2, **a–d, e–h**), and invasive transitional cell carcinoma (cases 3 and 4, **i–l**, **m–p**). Each of the four panels (**a–d**, **e–h**, **i–j**, **m–p**) shows normal and CIS or cancer tissues obtained from the same patient. Magnification ×10. Data are summarized in Fig. 7

fluorescence immunostaining and two by the $P2X_7$ receptor HRP–DAB immunostaining method. In seven of the 12 invasive ductal carcinomas, $P2X_7$ receptor levels were lower in the cancer cells than in the normal cells (e.g., Figs. 5a, c, e, g and 7h); in three cases of the 12 invasive ductal carcinomas, $P2X_7$ receptor levels were similar in the cancer and normal cells (Fig. 7h), and in two cases, $P2X_7$ receptor levels were higher in the cancer cells than in the normal cells (Fig. 7h). In all three invasive lobular carcinomas, $P2X_7$ receptor levels were lower in the cancer cells than in the normal cells (e.g., Fig. 5i, k). For the entire breast group, the mean ratio of cancer/normal $P2X_7$ receptor levels was 0.67±0.33 (Fig. 7h, $p<0.01$). In the two invasive ductal carcinoma cases that were evaluated by HRP–DAB immunostaining, $P2X_7$ receptor levels were lower in the cancer cells than in the normal cells (e.g., Fig. 6e, f).

Colon In cross sections of the normal colon, $P2X_7$ immunoreactivity was localized mainly in the basolateral aspect of the mucosal cells, with minimal nuclear staining (Fig. 5m). In colon adenocarcinoma cells, the $P2X_7$ immunoreactivity was distributed throughout the cells, but it was predominantly cytoplasmic with minimal nuclear staining (Fig. 5o). Five clinical cases of adenocarcinoma were studied (Table 1), all by $P2X_7$ receptor immunofluo-

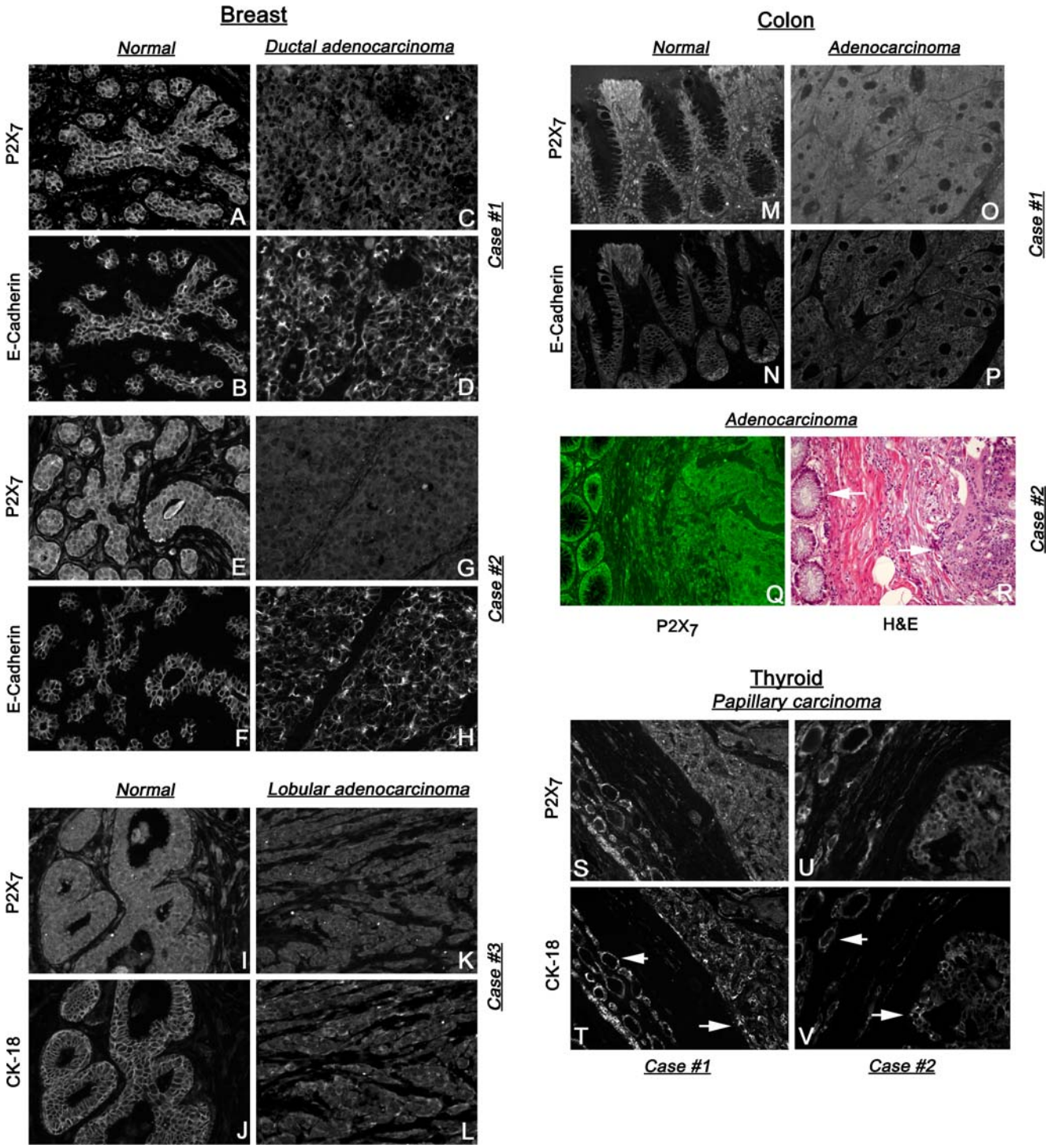

Fig. 5 $P2X_7$ and E-cadherin or cytokeratin-18 immunoreactivities (by immunofluorescence) in cross sections of normal and ductal adenocarcinoma breast tissues (**a–d**, **e–h**); normal and lobular adenocarcinoma breast tissues (**i–l**); normal and adenocarcinoma colon tissues (**m–p**, **q–r**); and normal and papillary carcinoma thyroid tissues (**s–v**). Each of the six panels (**a–d**, **e–h**, **i–l**, **m–p**, **q–r**, **s–v**) shows normal and cancer tissues obtained from the same patient. **q**, **r**, **s**, **t**, **u**, **v** Cross sections containing both normal (*left-pointed arrows*) and cancerous tissues (*right-pointed arrows*). Magnification ×10. Data are summarized in Fig. 7

rescence immunostaining. In all five cases, $P2X_7$ receptor levels were similar in the cancer cells and the normal cells (e.g., Fig. 5m, o, and q), with a mean ratio of cancer/normal $P2X_7$ receptor levels of 0.99±0.05 (Fig. 7k, $p>0.9$).

Thyroid In cross sections of the normal thyroid, $P2X_7$ immunoreactivity was localized mainly within thyrocytes bordering the follicles (Figs. 1e, 5s, u, and 6g, h); the immunoreactivity was most prominent at perinuclear

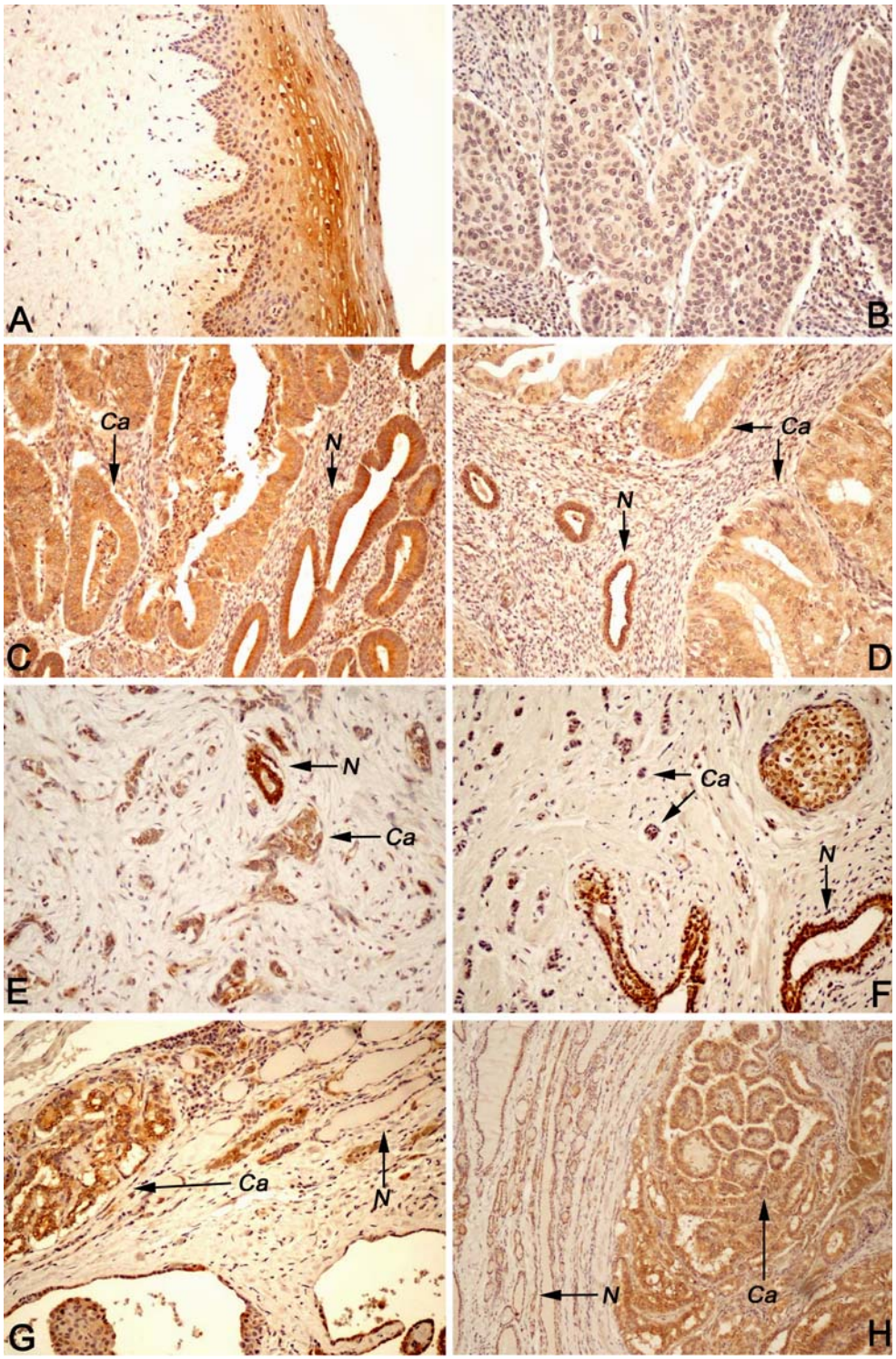

Fig. 6 $P2X_7$ immunoreactivity detected by HRP–DAB immunostaining (*brown color*), in cross sections of normal (**a**) and squamous cell carcinoma cervical tissues (**b**); endometrial tissues (**c**, **d**) containing both normal glands (*N*) and adenocarcinomatous glands (*Ca*); breast tissues (**e**, **f**) containing both normal ducts and ductal adenocarcinomatous tissues; and thyroid tissues (**g**, **h**) containing both normal and papillary carcinoma tissues. Magnification ×10

regions, but it was also found in the cytoplasm and plasma membrane regions (e.g., Fig. 5s). In thyroid papillary cancer cells, the $P2X_7$ immunoreactivity was distributed throughout the cells, with minimal nuclear staining (Figs. 5s, u and 6g, h). Four clinical cases of papillary carcinoma were studied (Table 1), all evaluated both by $P2X_7$ receptor immunofluorescence immunostaining and the $P2X_7$ receptor HRP–DAB immunostaining method. In all cases, $P2X_7$ receptor levels were higher in the cancer cells than in the normal cells (Fig. 5s, u), with a mean ratio of cancer/normal $P2X_7$ receptor levels of 1.26±0.16 (Fig. 7l, $p<0.01$). Similar results were obtained in the cancer cases that were evaluated by HRP–DAB immunostaining (e.g., Fig. 6g, h).

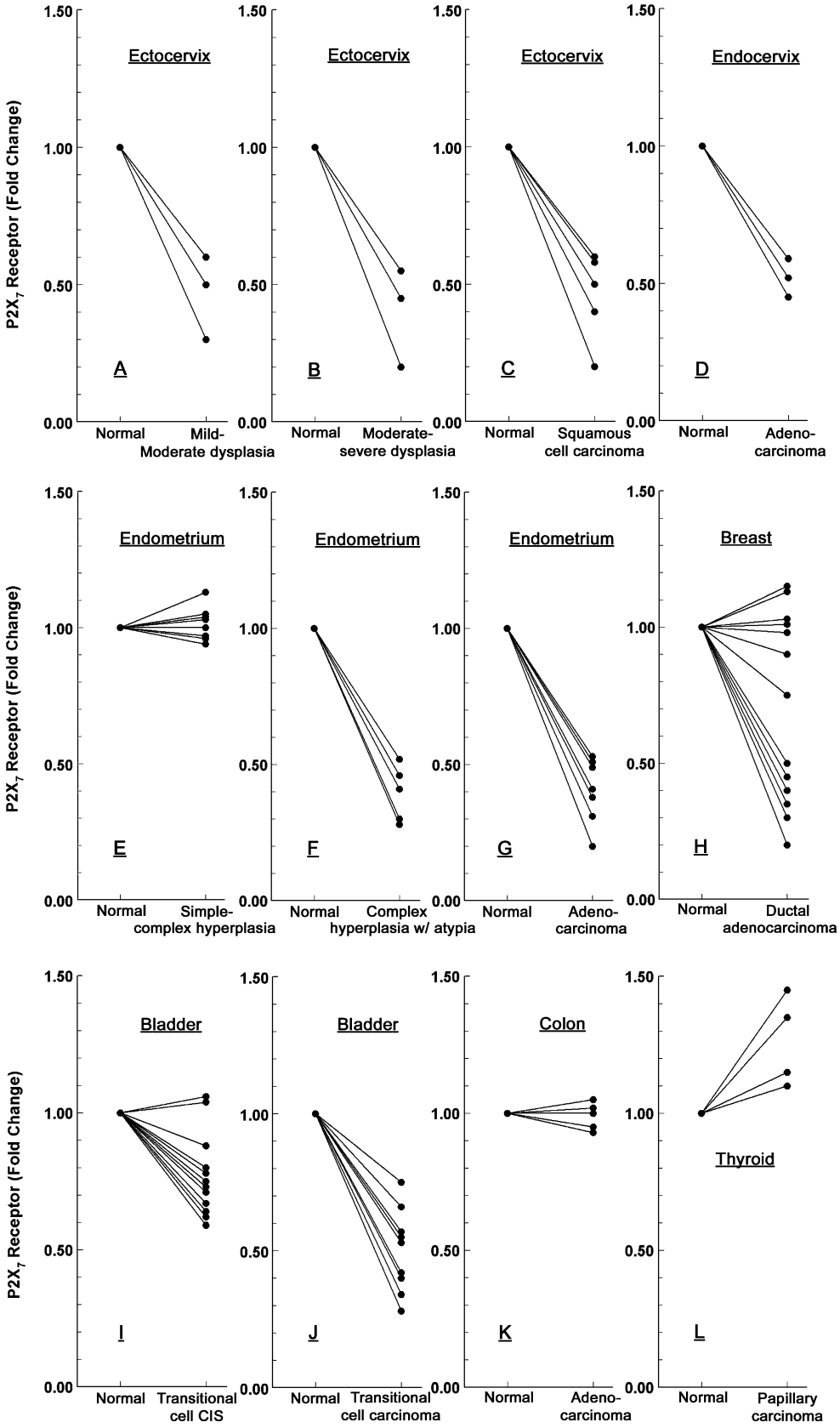

Fig. 7 a–l Summary of $P2X_7$ receptor immunofluorescence immunostaining data. *Each line* shows data determined in normal and abnormal tissues of the same clinical case

In summary, assays using two different immunostaining methods with anti-$P2X_7$ receptor antibodies that immunoreact with the functional, full-length $P2X_7$ receptor revealed lower levels of the $P2X_7$ receptor in ectocervical squamous cell carcinoma, endocervical and endometrial adenocarcinoma, bladder transitional cell carcinoma, and breast ductal and lobular carcinoma cells, than in the corresponding normal epithelial cells. In addition, $P2X_7$ receptor levels were lower also in dysplastic, pre-cancerous, and early cancerous epithelial cells of the ectocervix, endometrium, and bladder, compared to the corresponding normal epithelial cells. In thyroid papillary carcinoma cells, $P2X_7$ receptor levels were higher than in the corresponding normal epithelial cells, while $P2X_7$ receptor levels were similar in normal colon and adenocarcinoma epithelial cells.

$P2X_7$ mRNA levels in normal and cancer epithelial cells

To better understand the mechanism that leads to lower levels of the $P2X_7$ receptor in the uterine, bladder, and breast cancer epithelial cells, levels of $P2X_7$ mRNA were determined. For each clinical case (i.e., patient), minces containing the normal and abnormal tissues were processed and assayed simultaneously for $P2X_7$ mRNA steady-state levels by real-time qPCR (Table 1). C_t values (corresponding to total $P2X_7$ mRNA in the specimen) were normalized to E-cadherin mRNA (ectocervix and breast), or to cytokeratin-18 (CK-18) mRNA (endocervix, endometrium, and bladder) to determine the epithelium-related $P2X_7$ mRNA [33]. For each clinical case, data of epithelial $P2X_7$ mRNA levels in cancer tissues were normalized to those of normal cells.

For all five studied epithelia, $P2X_7$ mRNA steady-state levels were lower in the epithelial cancer component than in the normal epithelial tissues. Thus, the mean ratios of $P2X_7$/E-cadherin mRNA levels in cancer versus normal ectocervix and breast were 0.19 ± 0.08 and 0.51 ± 0.12, respectively (Fig. 8, $p<0.01$ [compared to normals]), and the mean ratios of $P2X_7$/CK-18 mRNA levels in cancer versus normal endocervix, endometrium, and bladder were 0.27 ± 0.14, 0.16 ± 0.06, and 0.08 ± 0.06, respectively (Fig. 8, $p<0.01$ [compared to normals]). These data indicate that in uterine, bladder, and breast cancer epithelial cells, low $P2X_7$ receptor levels correlate with low $P2X_7$ mRNA levels. Moreover, in those epithelia, the decrease of $P2X_7$ mRNA in cancer cells was quantitatively greater than that of the $P2X_7$ receptor.

Discussion

The main objective of the study was to better understand the biological role of $P2X_7$ in the genesis and development of epithelial cancers. The main findings were as follows: (a) Expression levels of the functional, full-length $P2X_7$ receptor in epithelial cancers are cell-type specific; (b) in uterine, bladder, and breast epithelial cancer cells, $P2X_7$ receptor and mRNA levels were lower than in the corresponding normal epithelial cells; (c) in the ectocervix endometrium and bladder, $P2X_7$ receptor levels were lower also in dysplastic, pre-cancerous, and early cancerous epithelial cells; and (d) $P2X_7$ receptor levels were higher in thyroid papillary carcinoma cells than in the corresponding normal epithelial cells and similar in colon adenocarcinoma and the corresponding normal epithelial cells.

The present data were obtained by two complementary immunostaining methods: immunofluorescence, which is more sensitive in capturing signals and therefore more amenable to quantification, and HRP–DAB which allows easier identification of tissue structural components. Data were similar regardless of the method used.

One of our objectives was to ascertain that the measured $P2X_7$ immunoreactivity reflects binding of the anti-$P2X_7$ receptor antibody to the functional form of the receptor. This is important for proper evaluation of the results, given the fact that conclusions of previous studies by others may have been influenced by the identification also of non-functional receptor(s). $P2X_7$ receptor polymorphism in reference to the functional full-length human $P2X_7$ (GeneBank accession number Y09561) involves mutated forms and variants (reviewed in [20]). All polymorphic forms resulting from point mutations can immunoreact with the presently used anti-$P2X_7$ receptor antibodies and provide theoretically inaccurate determinations for the expression of the functional $P2X_7$ receptor. However, studies in the lab found that the prevalence of normal or cancer cells bearing single nucleotide polymorphic forms in various epithelial tissues was low (not shown). Therefore, quantitatively, the presence of such forms should have had only a negligible effect on $P2X_7$ immunoreactivity with the use of the current anti-$P2X_7$ receptor antibodies.

In contrast and of greater concern are truncated variants of the human $P2X_7$ receptor, resulting from alternative splicing [20, 41, 42] that lack the carboxy terminus of the wild-type $P2X_7$ receptor. Since the carboxy terminus is essential for $P2X_7$ receptor-mediated apoptosis [20], these forms are non-functional. Of particular importance is the truncated $P2X_{7\text{-j}}$ isoform [20] that is prevalent in epithelial cancers including uterine [20], breast, bladder, skin, colon, and prostate (not shown). It is expressed in cancer epithelial cells at relatively high concentrations [20], and the expression ratio of the $P2X_{7\text{-j}}$ form compared to the full-length $P2X_7$ receptor is significantly higher in cancer epithelial cells than in the corresponding normal epithelial cells [20]. The $P2X_{7\text{-j}}$ form is ineffective when expressed

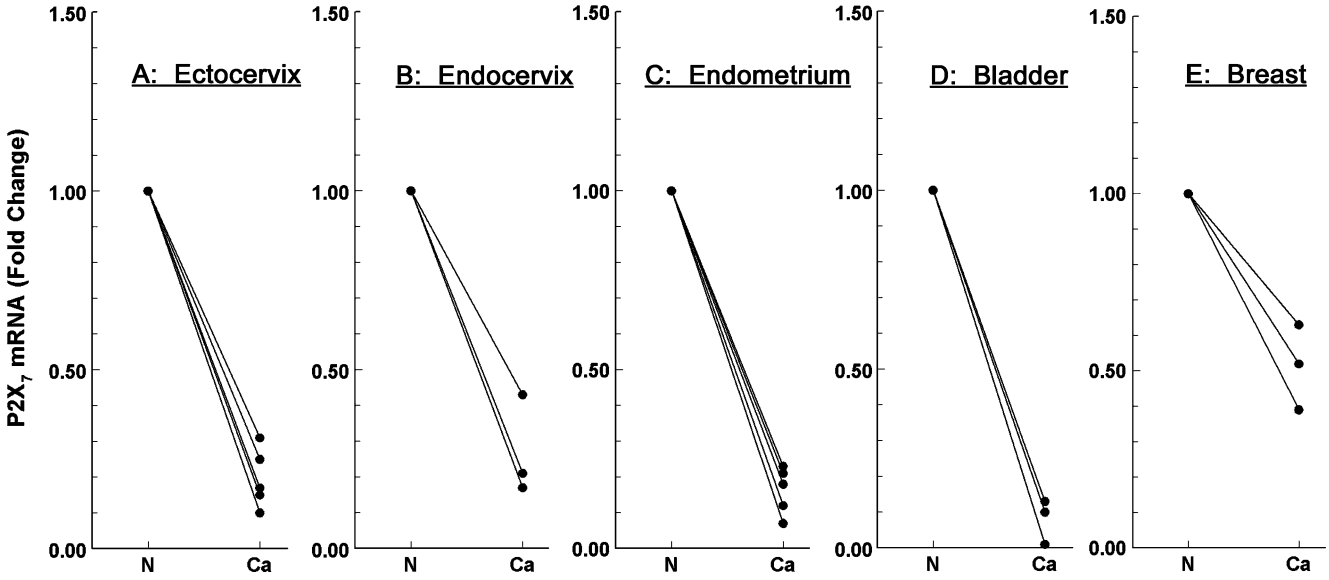

Fig. 8 **a**–**e** $P2X_7$ mRNA levels (by qPCR). *Each line* shows data determined in normal and abnormal tissues of the same clinical case

alone [20]. Moreover, when co-expressed with the functional full-length $P2X_7$ receptor, it can oligomerize and render it ineffective [20]. We therefore utilized anti-$P2X_7$ receptor antibodies that bind the full-length form but not truncated isoform(s) lacking the carboxy terminus of the receptor. These antibodies were previously shown to specifically interact with the functional full-length receptor, with only minimal influence by the expression of the $P2X_{7\text{-}j}$ variant [20, 26].

Depending on the type of cell that was studied, $P2X_7$ immunoreactivity could be found in different cellular locations. Co-localization with plasma membrane domains reflects the full-length, glycosylated active receptor inserted in the plasma membrane [20, 26]. $P2X_7$ immunoreactivity found in the cytoplasm may reflect newly formed receptor en route to be inserted into the plasma membrane, or post-activation internalized, degraded, or recycled receptor [20]. Perinuclear/nuclear $P2X_7$ immunoreactivity was previously described in epithelial [28, 43, 44] and other types of cells [45, 46], but its biological significance remains unclear. It is unlikely an artifact (i.e., non-specific binding) because it was found in tissues processed in parallel with those not found to express this type of signal (present study).

The present data in uterine epithelia confirmed previous reports [7, 33], with the novelty of presenting a more comprehensive and unified quantitative analysis and comparing data of $P2X_7$ immunofluorescence with $P2X_7$ HRP–DAB immunostaining. The data in normal endometrial glands also showed for the first time sorting of the $P2X_7$ receptor into apical domains of the plasma membrane, and the effect depended on the level of tissue differentiation. Accordingly, the degree of $P2X_7$ receptor sorting into apical regions of the plasma membrane was greatest in tissues of women at the late proliferative phase of the menstrual cycle (Fig. 1g–j). Previous studies also reported preferential sorting of the $P2X_7$ receptor into apical domains of the plasma membrane in cervical epithelial cells [40], as well as of other purinergic receptors ($P2Y_2$ and $P2X_4$ [47–50]). However, the biological significance of these findings is at present unclear.

The data in urinary bladder epithelial cells are novel, and they showed similar trends of lower $P2X_7$ receptor expression in cancer than in normal epithelial cells. Our data of higher $P2X_7$ receptor expression in thyroid papillary cancer cells than in normal thyroid epithelial cells confirm a recent report by Solini et al. [34].

The present breast data differ from those previously reported by Slater et al. [30]. The latter reported that normal and mildly hyperplastic breast epithelia were devoid of the $P2X_7$ receptor, whereas epithelial cells of in situ or invasive lobular or ductal carcinoma were labeled intensely. However, the assay used by Slater et al. [30] most likely identified non-functional splice variant(s) of the receptor [32]. The focus of the present study was evaluation of expression of the functional, full-length receptor, which mediates the apoptosis. Our data in normal breast tissues showed extensive expression of the functional $P2X_7$ receptor in ducts and acini (Fig. 5) and lowered expression in ductal and lobular cancer epithelial cells (Fig. 7h). Therefore, the most likely explanation for the differences between the present data and those of Slater et al. [30] is that normal breast epithelial cells express predominantly the functional full-length $P2X_7$ receptor, and that the expression of the receptor is decreased in cancer cells. In contrast, cancer cells express predominantly non-active variant(s), similar to previously reported data in the uterus [20].

The expression pattern of $P2X_7$ receptors in other types of epithelial cancers is at present unknown. Using a method that detected also non-functional receptor(s), Slater et al. [31] reported that $P2X_7$ receptors were absent from normal prostate epithelium, but were present in prostate cancers. However, $P2X_7$ immunoreactivity was present in apparently normal epithelial cells in acini well outside the tumor margins. Similarly, this group also reported extensive $P2X_7$ immunoreactivity in areas affected by spreading skin melanoma cells which extended 2 μm from the melanoma into the keratinocyte layer of the adjacent normal epidermis [29]. In view of the above discussion, those data need to be confirmed using assays that detect the functional form of the receptor.

A different trend, resembling that found by us in the uterus, bladder, and breast, was found by Greig et al. [28] in non-melanoma skin lesions. Their assay included the use of a polyclonal anti-$P2X_7$ receptor antibody raised against antigenic domain in the C-terminus of the receptor [51]. $P2X_7$ receptors were expressed in the stratum corneum of the epidermis, but only weakly in occasional squamous carcinoma cells and in necrotic regions within basal cell carcinoma tumors. In those tissues, the $P2X_7$ immunoreactivity co-localized with TUNEL labeling [28]. Their analysis of $P2X_7$ expression in different subgroups of basal cell carcinomas suggested that in moderately aggressive tumors there was a high level of expression of $P2X_7$ receptors, but with increasing aggressiveness of tumor this trend was reduced. Since apoptosis plays an important role in the tumorigenesis of basal cell carcinoma [28], the authors proposed that the loss of $P2X_7$ receptor expression could lead to increased tumor aggressiveness [28].

While our data in the uterus, bladder, and breast resemble those of Greig et al. [28], there is a fundamental difference between the results as they relate to the localization of $P2X_7$ immunoreactivity in normal stratifying epithelia. Stratified epithelia are composed of proliferating and regenerating cells of the basal layer which rest on the basal membrane and continue to divide throughout life. In the skin, a large pool of reserve cells can be also found in proliferating cells within hair shafts. Daughter cells in the parabasal layers differentiate into polyhedral cells that are most active in protein synthesis [52] and express early differentiation markers. Superficial to the parabasal layer are the granular layer of metabolically active cells, and the transitional layer of still living cells with evidence of early stages of terminal differentiation. The skin, in contrast to non-keratinizing stratified epithelia (e.g., the cervix), also contains the superficial stratum corneum, composed of layer(s) of flat dead cells [53].

The skin data of Greig et al. [28] identified intense $P2X_7$ immunoreactivity in the granular and transitional layers and in the stratum corneum. In contrast, they reported low $P2X_7$ immunoreactivity in basal/parabasal layers and only occasionally in hair follicles and mature hair shafts [28]. Similarly, in the non-keratinizing stratified epithelia of the cornea and esophagus, the authors found only little or no $P2X_7$ immunoreactivity [28]. Contrary to their findings, recent data [7, 33] and the present study localized intense $P2X_7$ immunoreactivity in human stratified epithelia in basal/parabasal layers (e.g., Fig. 2a). Our experiments, which probably utilized a more sensitive assay than that of Greig et al. also showed lesser expression in the intermediate ectocervical layers of the epithelium (equivalent to the epidermal granular layers) and more intense immunoreactivity in the superficial layers ([7]; Fig. 2a, e). The explanation to this undulant pattern of $P2X_7$ immunoreactivity is provided by the recent in situ hybridization assays in the normal human ectocervical epithelium [7]. The data showed that $P2X_7$ mRNA localized foremost to the basal/parabasal layers [7], in correlation with the intense $P2X_7$ immunoreactivity in those layers (Fig. 2a, e). In contrast, the $P2X_7$ immunoreactivity in the intermediate layers and the intense immunoreactivity in the superficial layers were not associated with de novo translated receptor protein [7]. Therefore, the receptor that is present in the metabolically active but non-proliferating granular (skin) and intermediate layers (in the ectocervix), and in cells in the more superficial layers, represents receptor trapped in dying cells that undergo terminal differentiation. These cells start to lose their cytoplasm, and as they flatten, the density of the retained $P2X_7$ immunoreactivity increases (e.g., Fig. 6a). From a biological point of view, the $P2X_7$ receptor in those cells could function to mediate apoptosis associated with terminal differentiation. However, this is a secondary function compared to its main role, which is regulation of growth of the proliferating cells in the basal/parabasal layers (and in hair shafts in the skin). These proliferating cells are the target of carcinogenic stimuli and are at risk of undergoing the neoplastic transformation. Our previous [7] and present data that the $P2X_7$ receptor is expressed by proliferating epithelial cells support the hypothesis that $P2X_7$ plays an important role in the regulation and control of growth of epithelial cells.

Based on these data, it is proposed that epithelia can be characterized according to the pattern of $P2X_7$ expression in normal and cancer cells: (a) epithelia with a similar trend of expression in normal and cancer cells, e.g., the colon (present data), in which the role of $P2X_7$ in the genesis and development of the cancer is relatively small; (b) epithelia with high expression of the $P2X_7$ in cancer cells, e.g., thyrocytes—Whether in those cases the cancer cells overproduce the receptor as an inherent growth protective mechanism, or whether the $P2X_7$ stimulates proliferation [34], remains to be determined; and (c) epithelia in which $P2X_7$ expression is decreased already in early phases of the

neoplasia, e.g., the uterine epithelia, bladder, and breast. This could abrogate apoptosis and lead to unstable tissue kinetics, favoring an increase in total cell number and tumor cellular expansion in cells exposed to the carcinogenic stimulus [28]. One possibility is that the neoplastic stimulus triggers decreased expression of the $P2X_7$, thereby contributing to uncontrolled cell growth. The present data in endometrial and bladder cells of low expression of the $P2X_7$ receptor already in pre-cancerous and early cancerous cells support this hypothesis. However, a more fundamental possibility is that the decrease in $P2X_7$ expression occurs prior to the neoplastic transformation, as was observed in cases of cervical dysplasia (e.g., Fig. 1c, g), where the abrogation of $P2X_7$-mediated apoptosis could be responsible for the preservation of genetically aberrant cells that are susceptible to carcinogenic stimuli, favoring neoplastic transformation [54]. In the cervix, virulent human papilloma viruses (HPV) contribute to the development of dysplasia and possibly squamous cell carcinoma [55]. However, only few cases of dysplasia progress to cancer [55]. The present data showed that decreased expression of the $P2X_7$ was observed already in cases of mild-moderate dysplasia, which usually do not transform into cancer. Therefore, it is possible that in the cervix the decreased expression of the $P2X_7$ precedes the carcinogenic stimulus, thereby increasing the risk of neoplastic transformation of HPV-infected cells.

Collectively, our past and present observations and the data of Greig et al. [28] support the hypothesis that in the uterus, bladder, breast, and skin the $P2X_7$ mechanism plays a physiological role in the control of epithelial cell growth. The data suggest an embryologic background to the tissue-specific expression of the $P2X_7$. Accordingly, in cancer cells of epithelia derived from the endoderm (thyroid and colon), $P2X_7$ receptors levels are higher or equal to those in normal cells. In contrast, in cancer cells of epithelia derived from the ectoderm (skin and breast), the uro-genital sinus (bladder and ectocervix), and the distal paramesonephric (Müllerian) duct (endocervix and endometrium), $P2X_7$ receptors levels are low. It is therefore possible that early embryonic events imprint $P2X_7$ expression in the later stage of life.

The mechanism that determines low expression of $P2X_7$ receptor in uterine, bladder, breast, and possibly skin epithelial cancer cells is at present unknown. $P2X_7$ mRNA steady-state levels in these epithelia were also low in the cancer tissues (present data and unpublished data [skin]), suggesting an effect already at the mRNA level. Since the decrease of $P2X_7$ mRNA in cancer cells was quantitatively greater than that of the $P2X_7$ receptor, the effect most likely is not translational. More likely, based on a recent study [25], the effect is post-transcriptional, involving enhanced instability of the 3′ untranslated region (3′-UTR) of the $P2X_7$ gene, through the action of micro-RNAs (miRNAs). In the human cervix and endometrium, miRNAs miR-150 and miR-186 were identified as two factors that regulate $P2X_7$ 3′-UTR, and cellular levels of these miRNAs were higher in the cancer than normal epithelial cells. However, little is known about the role of miRNAs in the regulation $P2X_7$ 3′-UTR in the bladder, breast, and skin epithelia.

In summary, we found decreased expression of the functional full-length $P2X_7$ receptor in cancer cells of epithelia derived from the ectoderm, the uro-genital sinus, and the distal paramesonephric duct. In the ectocervix endometrium and bladder, $P2X_7$ receptor levels were lower also in dysplastic, pre-cancerous, and early cancerous epithelial cells. Since $P2X_7$-mediated apoptosis is an important mechanism that regulates epithelial cell growth, it is possible that early embryonic events imprint $P2X_7$ expression in the later stage of life and confer the risk of cancer development in those tissues.

Acknowledgment The study was supported in part by NIH grant AG15955 and by an unrestricted grant by CytoCore Inc. to GIG.

Conflict of interest CytoCore Inc. funded a small part of the study but it has no financial interest in the study. Dr. Gorodeski was paid consultant to CytoCore Inc. and he holds restricted stocks of CytoCore. The ties between Dr. Gorodeski and CytoCore were severed in March 2008, prior to completion of the study, and Dr. Gorodeski has no financial interest in the study. None of the other authors had any ties with CytoCore. Neither Dr. Gorodeski, nor any of the other authors have other financial or non-financial competing interests. None of the authors hold any patents related to the study. University Hospital CASE Medical Center and Case Western Reserve University have a financial interest in the study.

References

1. Wyllie AH, Kerr JFR, Currie AR (1980) Cell death: the significance of apoptosis. Int Rev Cytol 68:251–306. doi:10.1016/S0074-7696(08)62312-8
2. Ellis HM, Yuan J, Horvitz HR (1991) Mechanisms and functions of cell death. Annu Rev Cell Biol 7:663–698. doi:10.1146/annurev.cb.07.110191.003311
3. Fawthrop DJ, Boobis AR, Davies DS (1991) Mechanisms of cell death. Arch Toxicol 65:437–444. doi:10.1007/BF01977355
4. Soti C, Sreedhar AS, Csermely P (2003) Apoptosis, necrosis and cellular senescence: chaperone occupancy as a potential switch. Aging Cell 2:39–45. doi:10.1046/j.1474-9728.2003.00031.x
5. Renvoize C, Biola A, Pallardy M, Breard J (1998) Apoptosis: identification of dying cells. Cell Biol Toxicol 14:111–120. doi:10.1023/A:1007429904664
6. Wang Q, Wang L, Feng YH, Li X, Zeng R, Gorodeski GI (2004) $P2X_7$-receptor mediated apoptosis of human cervical epithelial cells. Am J Physiol 287:C1349–C1358. doi:10.1152/ajpcell.00256.2004
7. Li X, Zhou L, Feng YH, Abdul-Karim F, Gorodeski GI (2006) The $P2X_7$ receptor: a novel biomarker of uterine epithelial cancers. Cancer Epidemiol Biomarkers Prev 15:1–8. doi:10.1158/1055-9965.EPI-05-0923

8. Dubyak GR, el-Moatassim C (1993) Signal transduction via P2-purinergic receptors for extracellular ATP and other nucleotides. Am J Physiol 265:C577–C606
9. Ralevic V, Burnstock G (1998) Receptors for purines and pyrimidines. Pharmacol Rev 50:413–492
10. North RA (2002) Molecular physiology of P2X receptors. Physiol Rev 82:1013–1067
11. Sperlágh B, Haskó G, Németh Z, Vizi ES (1998) ATP released by LPS increases nitric oxide production in raw 264.7 macrophage cell line via P2Z/P2X7 receptors. Neurochem Int 33:209–215. doi:10.1016/S0197-0186(98)00025-4
12. Grahames CBA, Michel AD, Chessell IP, Humphrey DPA (1999) Pharmacological characterization of ATP- and LPS-induced IL-1β release in human monocytes. Br J Pharmacol 127:1915–1921. doi:10.1038/sj.bjp.0702732
13. Henriksen KL, Novak I (2003) Effect of ATP on intracellular pH in pancreatic ducts involves P2X7 receptors. Cell Physiol Biochem 13:93–102. doi:10.1159/000070253
14. Loomis WH, Namiki S, Ostrom RS, Insel PA, Junger WG (2003) Hypertonic stress increases T-cell Interleukin-2 expression through a mechanism that involves ATP release, P2 Receptor, and p38 MAPK activation. J Biol Chem 278:4590–4596. doi:10.1074/jbc.M207868200
15. Wang Q, Li X, Wang L, Feng YH, Zeng R, Gorodeski GI (2004) Anti-apoptotic effects of estrogen in normal and in cancer human cervical epithelial cells. Endocrinology 145:5568–5579. doi:10.1210/en.2004-0807
16. Ferrari D, Chiozzi P, Falzoni S, Dal Susino M, Melchiorri L, Baricordi OR et al (1997) Extracellular ATP triggers IL-1β release by activating the purinergic P2Z receptor of human macrophages. J Immunol 159:1451–1458
17. Aggarwal BB, Rath PC (1999) TNF-induced signaling in apoptosis. J Clin Immunol 19:350–364. doi:10.1023/A:1020546615229
18. Humphreys BJ, Rice J, Kertesy SB, Dubyak GR (2000) Stress-activated protein kinase/JNK activation and apoptotic induction by the macrophage $P2X_7$ nucleotide receptor. J Biol Chem 275:26792–26798
19. Ferrari D, Wesselborg S, Bauer MK, Schulze-Osthoff K (1997) Extracellular ATP activates transcription factor NF-κB through the P2Z purinoreceptor by selectively targeting NF-κB p65. J Cell Biol 139:1635–1643. doi:10.1083/jcb.139.7.1635
20. Feng YH, Li X, Wang L, Zhou L, Gorodeski GI (2006) A truncated $P2X_7$ receptor variant ($P2X_{7\text{-}j}$) endogenously expressed in cervical cancer cells antagonizes the full-length $P2X_7$ receptor through hetero-oligomerization. J Biol Chem 281:17228–17237. doi:10.1074/jbc.M602999200
21. Locovei S, Scemes E, Qiu F, Spray DC, Dahl G (2007) Pannexin1 is part of the pore forming unit of the P2X7R death complex. FEBS Lett 581:483–488. doi:10.1016/j.febslet.2006.12.056
22. Iglesias R, Locovei S, Roque A, Alberto AP, Dahl G, Spray DC et al (2008) $P2X_7$ receptor–Pannexin1 complex: pharmacology and signaling. Am J Physiol 295:C752–C760. doi:10.1152/ajpcell.00228.2008
23. Kim M, Spelta V, Sim J, North RA, Surprenant A (2001) Differential assembly of rat purinergic P2X7 receptor in immune cells of the brain and periphery. J Biol Chem 276:23262–23267. doi:10.1074/jbc.M102253200
24. Guo C, Masin M, Qureshi OS, Murrell-Lagnado RD (2007) Evidence for functional P2X4/P2X7 heteromeric receptors. Mol Pharmacol 72:1447–1456. doi:10.1124/mol.107.035980
25. Zhou L, Qi X, Potashkin JA, Abdul-Karim FW, Gorodeski GI (2008) MicroRNAs miR-186 and miR-150 down-regulate expression of the pro-apoptotic purinergic $P2X_7$ receptor by activation of instability sites at the 3′-untranslated region of the gene that decrease steady-state levels of the transcript. J Biol Chem 283:28274–28286. doi:10.1074/jbc.M802663200
26. Feng YH, Wang L, Wang Q, Li X, Zeng R, Gorodeski GI (2005) ATP stimulates GRK-3-phosphorylation and β-arrestin-2-dependent internalization of the P2X7-receptor. Am J Physiol 288:C1342–C1346. doi:10.1152/ajpcell.00315.2004
27. Wang L, Feng YH, Gorodeski GI (2005) EGF facilitates epinephrine inhibition of $P2X_7$-receptor mediated pore formation and apoptosis: a novel signaling network. Endocrinology 146:164–174. doi:10.1210/en.2004-1026
28. Greig AV, Linge C, Healy V, Lim P, Clayton E, Rustin MH et al (2003) Expression of purinergic receptors in non-melanoma skin cancers and their functional roles in A431 cells. J Invest Dermatol 121:315–327. doi:10.1046/j.1523-1747.2003.12379.x
29. Slater M, Scolyer RA, Gidley-Baird A, Thompson JF, Barden JA (2003) Increased expression of apoptotic markers in melanoma. Melanoma Res 13:137–145. doi:10.1097/00008390-200304000-00005
30. Slater M, Danieletto S, Pooley M, The LC, Gidley-Baird A, Barden JA (2004) Differentiation between cancerous and normal hyperplastic lobules in breast lesions. Breast Cancer Res Treat 83:1–10. doi:10.1023/B:BREA.0000010670.85915.0f
31. Slater M, Danieletto S, Gidley-Baird A, The LC, Barden JA (2004) Early prostate cancer detected using expression of non-functional cytolytic $P2X_7$ receptors. Histopathology 44:206–215. doi:10.1111/j.0309-0167.2004.01798.x
32. Barden JA, Sluyter R, Gu BJ, Wiley JS (2003) Specific detection of non-functional human $P2X_7$ receptors in HEK293 cells and B-lymphocytes. FEBS Lett 538:159–162. doi:10.1016/S0014-5793(03)00172-8
33. Li X, Qi X, Zhou L, Catera D, Rote NS, Potashkin J et al (2007) Decreased expression of $P2X_7$ in endometrial epithelial pre-cancerous and cancer cells. Gynecol Oncol 106:233–243. doi:10.1016/j.ygyno.2007.03.032
34. Solini A, Cuccato S, Ferrari D, Santini E, Gulinelli S, Callegari MG et al (2008) Increased $P2X_7$ receptor expression and function in thyroid papillary cancer: a new potential marker of the disease? Endocrinology 149:389–396. doi:10.1210/en.2007-1223
35. Gasser S, Raulet D (2006) The DNA damage response, immunity and cancer. Semin Cancer Biol 16:344–347. doi:10.1016/j.semcancer.2006.07.004
36. Kujoth GC, Leeuwenburgh C, Prolla TA (2006) Mitochondrial DNA mutations and apoptosis in mammalian aging. Cancer Res 66:7386–7389. doi:10.1158/0008-5472.CAN-05-4670
37. Rodriguez-Nieto S, Zhivotovsky B (2006) Role of alterations in the apoptotic machinery in sensitivity of cancer cells to treatment. Curr Pharm Des 12:4411–4425. doi:10.2174/138161206779010495
38. Surprenant A, Rassendren F, Kawashima E, North RA, Buell G (1996) The cytolytic P2Z receptor for extracellular ATP identified as a P2X receptor ($P2X_7$). Science 272:735–738. doi:10.1126/science.272.5262.735
39. Buell GN, Talabot F, Gos A, Lorenz J, Lai E, Morris MA et al (1998) Gene structure and chromosomal localization of the human $P2X_7$ receptor. Receptors Channels 5:347–354
40. Li X, Gorodeski GI (2006) Apically sorted P2X7 receptors mediate purinergic-induced pore formation preferentially in apical domains of the plasma membrane. Nucleosides Nucleotides Nucleic Acids 25:1045–1049. doi:10.1080/15257770600890913
41. Cheewatrakoolpong B, Gilchrest H, Anthes JC, Greenfeder S (2005) Identification and characterization of splice variants of the human $P2X_7$ ATP channel. Biochem Biophys Res Commun 332:17–27. doi:10.1016/j.bbrc.2005.04.087
42. Georgiou JG, Skarratt KK, Fuller SJ, Martin CJ, Christopherson RI, Wiley JS et al (2005) Human epidermal and monocyte-derived langerhans cells express functional P2X receptors. J Invest Dermatol 125:482–490. doi:10.1111/j.0022-202X.2005.23835.x

43. Lee HY, Bardini M, Burnstock G (2000) Distribution of P2X receptors in the urinary bladder and the ureter of the rat. J Urol 163:2002–2007. doi:10.1016/S0022-5347(05)67618-5
44. Menzies J, Paul A, Kennedy C (2003) $P2X_7$ subunit-like immunoreactivity in the nucleus of visceral smooth muscle cells of the guinea pig. Auton Neurosci Basic Clin 106:103–109. doi:10.1016/S1566-0702(03)00078-X
45. Franke H, Gunther A, Grosche J, Schmidt R, Rossner S, Reinhardt R et al (2004) $P2X_7$ receptor expression after ischemia in the cerebral cortex of rats. J Neuropathol Exp Neurol 636:86–99
46. Jiang LH, Kim M, Spelta V, Bo X, Surprenant A, North RA (2003) Subunit arrangement in P2X receptors. J Neurosci 23:8903–8910
47. Gorodeski GI, Hopfer U, De Santis BJ, Eckert RL, Rorke ER, Utian WH (1995) Biphasic regulation of paracellular permeability in human cervical cells by two distinct nucleotide receptors. Am J Physiol 268:C1215–C1226
48. Gorodeski GI, Hopfer U, Wenwu J (1998) Purinergic receptor induced changes in paracellular resistance across cultures of human cervical cells are mediated by two distinct cytosolic calcium related mechanisms. Cell Biochem Biophys 29:281–306. doi:10.1007/BF02737899
49. Gorodeski GI (2002) Regulation of transcervical permeability by two distinct P2-purinergic receptor mechanisms. Am J Physiol 282:C75–C83
50. Gorodeski GI (2002) Expression regulation and function of $P2X_4$ receptor in human cervical epithelial cells. Am J Physiol 282: C84–C93
51. Gröschel-Stewart U, Bardini M, Robson T, Burnstock G (1999) Localization of $P2X_5$ and $P2X_7$ receptors by immunohistochemistry in rat stratified squamous epithelia. Cell Tissue Res 296:599–605. doi:10.1007/s004410051321
52. Stern JB, Sekeri-Pataryas KH (1972) The uptake of 14C-leucine and 14C-histidine by cell suspensions of isolated strata of neonatal rat epidermis. J Invest Dermatol 59:251–259. doi:10.1111/1523-1747.ep12627274
53. Eckert RL, Crish JF, Robinson NA (1997) The epidermal keratinocyte as a model for the study of gene regulation and cell differentiation. Physiol Rev 77:397–424
54. Staibano S, Muzio LL, Mezza E, Argenziano G, Tornillo L, Pannone G et al (1999) Prognostic value of apoptotic index in cutaneous basal cell carcinomas of head and neck. Oral Oncol 35:541–547. doi:10.1016/S1368-8375(99)00028-7
55. Walboomers JM, Jacobs MV, Manos MM, Bosch FX, Kummer JA, Shah KV, Snijders PJ, Peto J, Meijer CJ, Muñoz N (1999) Human papillomavirus is a necessary cause of invasive cervical cancer worldwide. J Pathol 189:12–19. doi:10.1002/(SICI)1096-9896(199909)189:1<12::AID-PATH431>3.0.CO;2-F